8-2013

TYPE II CEPHEID CANDIDATES. IV. OBJECTS FROM THE NORTHERN SKY VARIABILITY SURVEY

Edward G. Schmidt
University of Nebraska-Lincoln, eschmidt1@unl.edu

The Astronomical Journal, 146:61 (13pp), 2013 September doi:10.1088/0004-6256/146/3/61

TYPE II CEPHEID CANDIDATES. IV. OBJECTS FROM THE NORTHERN SKY VARIABILITY SURVEY

Edward G. Schmidt[1]
Department of Physics and Astronomy, University of Nebraska, Lincoln, NE, USA; eschmidt1@unl.edu
Received 2013 March 19; accepted 2013 May 10; published 2013 August 9

ABSTRACT

We have obtained *VR* photometry of 447 Cepheid variable star candidates with declinations north of −14°30′, most of which were identified using the Northern Sky Variability Survey (NSVS) data archive. Periods and other photometric properties were derived from the combination of our data with the NSVS data. Atmospheric parameters were determined for 81 of these stars from low-resolution spectra. The identification of type II Cepheids based on the data presented in all four papers in this series is discussed. On the basis of spectra, 30 type II Cepheids were identified while 53 variables were identified as cool, main sequence stars and 283 as red giants following the definitions in Paper III. An additional 30 type II Cepheids were identified on the basis of light curves. The present classifications are compared with those from the Machine-learned All Sky Automated Survey Classification Catalog for 174 stars in common.

Key words: stars: Population II – stars: variables: Cepheids

Online-only material: machine-readable and VO tables

1. INTRODUCTION

This is the fourth and final paper in a series reporting the results of a project originally intended to greatly increase the number of type II Cepheids known. The goal was to discover objects that could contribute to a variety of astrophysical areas including studies of the structure of the galactic thick disk and halo, stellar pulsation, and the late stages of stellar evolution. Schmidt et al. (2007, Paper I) can be consulted for further information regarding the background of this project.

Paper I and Schmidt et al. (2009, 2011, Papers II and III) reported photometry and spectroscopy for Cepheid candidates selected from Akerlof et al. (2000) and Pojmanski et al. (2005). These catalogs were based on the Northern Sky Variability Survey (NSVS) and the All Sky Automated Survey (ASAS).

As the project progressed, many fewer type II Cepheids were found than expected and many candidates turned out to be red-giant-branch or cool main-sequence stars. Additionally, small amplitude variables were found to be more abundant than expected. Thus, the original goals of the project were broadened to include characterizing the nature of other stars with Cepheid-like periods.

The present paper extends this project to areas of the sky not included previously. In Section 2 we describe the selection of stars while the new observations are discussed in Section 3. Section 4 presents the parameters derived from the observations and Section 5 discusses the identification of Cepheids and provides a definitive list of the type II Cepheids found in this series of papers. Finally, in Section 6 we present the overall conclusions from the four papers in this series.

2. THE SAMPLE SELECTION

2.1. The NSVS Public Data Release

The NSVS Public Data Release[2] (Wozniak et al. 2004) contains light curves for about 14 million objects spanning one year. We searched this database for variables in the Cepheid period range, from 1.01 to 100 days, with declinations between +28° and +60°. This declination range was selected to cover most of the northern sky not included in Papers I and II. As explained in Paper I, we excluded stars within 10° of the Galactic Plane since we are searching for type II Cepheids.

The "rms_mag" column in the Object Table of the NSVS database lists the standard deviation of "good" points around the median magnitude for each star; denoted here by σ_{m_N}. In a plot of σ_{m_N} against the mean NSVS magnitude, denoted by $\langle m_N \rangle$, for 4000 stars from the table, a large majority fell along a well defined lower envelope of the distribution (as seen clearly in Figure 4 of Wozniak et al. 2004). We fitted the envelope with the polynomial

$$\sigma_{m_N,\mathrm{env}} = -4.557 + 1.2489\langle m_N \rangle - 0.11321\langle m_N \rangle^2 + .003416\langle m_N \rangle^3. \quad (1)$$

If we assume that this represents the observational uncertainty of an individual magnitude, then excess scatter,

$$\sigma_{m_N,\mathrm{var}} = \sqrt{\sigma^2_{m_N} - \sigma^2_{m_N,\mathrm{env}}}\,, \quad (2)$$

will likely be due to variability.

A preliminary list of candidates was obtained by selecting stars from the Object Table with more than 30 data points and $\sigma_{m_N,\mathrm{var}} > 0.10$. Periods were determined for all of these stars using the data-compensated discrete Fourier transform method of Ferraz-Mello (1981). Stars that lacked a significant period in the range from $P = 1.01$ to 100 days or had a more significant period shorter than this range were dropped from the list. The light curves for the more than 9600 remaining stars were then phased with the most significant periods and examined manually. For many stars, the majority of points were at a constant magnitude with a number of outliers. These are likely to be eclipsing binaries or stars with poor photometry so they were rejected. This step is highly subjective; we tried to err on the side of including dubious cases.

We filtered our remaining candidates using the General Catalogue of Variable Stars (GCVS; with corrections and

[1] Visiting Astronomer, Kitt Peak National Observatory, National Optical Astronomy Observatory, which is operated by the Association of Universities for Research in Astronomy, Inc., under cooperative agreement with the National Science Foundation.
[2] Available at http://skydot.lanl.gov/.

Table 1
The Program Stars and Photometric Parameters from the NSVS Photometry

No.	Sexagesimal Designation	Other Identifier	$\langle m \rangle$	Δm	σ_m	N_{obs} (NSVS)	Notes
(1)	(2)	(3)	(4)	(5)	(6)	(7)	(8)
B001	J000413.11+494214.7		13.11	0.55	0.06	59	a,d
B002	J000451.28+444440.3		10.49	0.33	0.06	90	a
B003	J000557.96+444947.7		11.92	0.37	0.07	94	a,h
B004	J001929.73+483830.4		11.68	0.38		304	c,d
B005	J002224.54+301251.5		11.72	0.43		286	c

Notes.
[a] $\langle m \rangle$ is the intensity mean over the cycle, Δm is the amplitude of a Fourier fit to the light curve, and σ_m is the rms scatter of the individual points about the Fourier fit. The period from Table 5 was used unless flagged by footnote g in this table.
[b] The variation in the NSVS data was judged to be of marginal significance; see the text for a discussion. $\langle m \rangle$ is the arithmetic mean of all the nightly mean magnitudes, and σ_m is the rms scatter about the mean magnitude. Δm is not listed.
[c] This star is a likely variable in the NSVS data but no meaningful period could be determined for the NSVS data, the variation was irregular or the phase coverage of the NSVS data was inadequate for a Fourier fit. $\langle m \rangle$ is the arithmetic mean of the all the nightly mean magnitudes, and Δm is the difference between the medians of the five faintest and five brightest magnitudes. No σ_m is given.
[d] See a note for this star in Table 11.
[e] One or a few anomalous magnitudes were deleted from the NSVS data before determining $\langle m \rangle$, Δm, and σ_m.
[f] Also identified by Hoffman et al. (2009).
[g] The NSVS period from Table 6 was used.
[h] There are two or more stars near the putative variable location on the sky. They are apparently blended in the NSVS photometry so $\langle m \rangle$ must be used with caution.

(This table is available in its entirety in machine-readable and Virtual Observatory (VO) forms in the online journal. A portion is shown here for guidance regarding its form and content.)

additions from the online version)[3] and photometry from the Two Micron All Sky Survey (hereafter 2MASS; Skrutskie et al. 2006). Stars found in the GCVS were eliminated from our program if they appeared to be well observed previously but were retained if it was judged that they might prove to be of interest with more observations. After matching our candidates with the 2MASS photometry, we eliminated stars with both $\langle m_N \rangle - K > 4.04$ and $J - K > 1.20$. These criteria are based on previous experience (Papers I and II) and, again, we tried to err on the side of inclusion.

Finally, a number of stars were found to lack suitable comparison stars or to be too bright to observe with our instrumentation. Our observations of the remaining stars are reported here.

2.2. Catalogs of Variables

Hoffman et al. (2009) identified and classified 4659 variable stars in the first NSVS data release (Wozniak et al. 2004). We selected stars from their Tables 2 (RR Lyr Candidates) and 3 (Cepheid/Long-Period Variable Candidates) with periods longer than 0.8 days, galactic latitudes greater than 10° and declinations north of −15°. Since the NSVS data spanned only one year, longer periods are uncertain. For this reason and to include any very long period Cepheids, we retained several stars for which Hoffman et al. (2009) listed periods between 100 and 154 days. We then removed stars from the list that were included in Papers I or II or that are well known Cepheids. Thirty-five stars were selected during the process described in Section 2.1 and are included among that group (as indicated by footnote f to Table 1). We removed stars that were too red as described above and a few stars were omitted due to a lack of usable comparison stars or for being too bright for our instrumentation.

Mondal et al. (2010) discovered 15 new variable star in data from the TAOS survey. Four of these, TAOS 151-01, TAOS 151-02, TAOS 151-03, and TAOS 151-04, meet our criteria for this project and are included here.

Wils & Greaves (2004) identified 40 new Cepheids from a search of the NSVS. The only star in their list with a galactic latitude greater than 10°, G2063 0653, was included in our program.

2.3. The Program Stars

The program stars are listed in Table 1 along with information derived from the NSVS database. The first column contains a running number for use in this paper. These numbers have prefixes of B, H, T, or W to indicate that they were selected from the NSVS database (as described in Section 2.1), Hoffman et al. (2009), Mondal et al. (2010), or Wils & Greaves (2004) respectively. The second column contains the sexagesimal designation of the star and the third column gives the designations from the GCVS, Hoffman et al. (2009), or Wils & Greaves (2004) for stars listed in those sources.

3. THE OBSERVATIONS

3.1. Photometry

We have obtained *VR* photometry for all the stars in Table 1. The new photometry and the existing NSVS photometry complement each other to allow a more thorough study of individual stars than could be accomplished by either alone. The extensive temporal coverage of the NSVS data gives a good picture of the short term stability of the variation. It was not possible to achieve comparable coverage from Behlen Observatory but the new photometry provides the colors and magnitudes of the stars on the standard system and greater accuracy for the fainter stars. The combination of both data sets allows the determination of more certain periods and the study of the pulsational behavior and stability over a longer time.

We made more than 6700 *RV* observations of the program stars between 2007 January 18 and 2012 May 14 (JD 2,454,119 − 2,456,062) at Behlen Observatory. The same instrumentation and procedures for collecting and processing the data were used as in Paper I and the reader is referred to that publication for details. The individual Behlen observations are listed in Table 2.

3.2. Spectroscopy

Spectra for 81 of the present program stars, two stars from Paper II that were not included in Paper III (A273 and A277), and 23 standard stars were obtained with the GoldCam spectrograph on the Kitt Peak National Observatory 2.1 m telescope during five nights in 2010 August. The same instrumental setup, and the same observation, reduction, and analysis procedures were used as for Paper III; that publication should be consulted for details.

LICK/IDS indices were calculated for each of our spectra. The 23 standard stars were used to derive transformations

[3] VizieR Online Data Catalog, II/214A.

Table 2
Photometric Data

Star	HJD −2,450,000	V	$V-R$
(1)	(2)	(3)	(4)
B001	4345.955	12.771	.385
B001	4434.742	13.246	.429
B001	4453.646	12.809	.400
B001	4464.618	12.977	.392
B001	4468.626	12.824	.391

(This table is available in its entirety in machine-readable and Virtual Observatory (VO) forms in the online journal. A portion is shown here for guidance regarding its form and content.)

between our indices and the MILES system and our indices were all transformed to that system. Table 3 lists the LICK/IDS indices for the individual spectra. Each spectrum is identified by the running number of the star in Column 1 and the HJD of mid-exposure in Column 2 while the remaining 26 columns give all of the LICK/IDS indices. It should be noted that in Table 2 of Paper III we listed the raw indices (and provided the transformation coefficients in Table 4) while here we tabulate the transformed indices.

Table 4 lists the atmospheric parameters derived from each program star spectrum. Again the spectra are identified in Columns 1 and 2 by the running number of the star and the HJD of mid-exposure. Columns 3, 4 and 5 give the effective temperature, $T_{\rm eff}$, the logarithm of the gravity, log g, and the metallicity, [Fe/H].

Intrinsic colors were calculated from $T_{\rm eff}$, log g, and [Fe/H] for each spectrum using the relations of VandenBerg and Clem (2003). Colors appropriate to the time of each spectrum, $(V-R)_\phi$, were estimated from the periods in Table 5 and the present photometry. The resulting color excesses are listed in Column 6 of Table 4. Period uncertainties, color curve scatter, sparse phase coverage, and irregular variation all introduce uncertainty into $(V-R)_\phi$. This uncertainty was assessed and if it affected the final mean color excess at a level greater than 0.02 mag, no color excesses are given for that star.

4. PROPERTIES DERIVED FROM THE OBSERVATIONS

4.1. The Periods

The periods of all the stars were determined in the same manner as in Paper I, Section 3.2 and Paper II, Section 2.3. In particular, a zero point was applied to the NSVS photometry

Table 4
The Atmospheric Parameters from Individual Spectra

Star	Mid Exposure HJD − 2,450,000	$T_{\rm eff}$[a]	log g	[Fe/H]	E_{V-R}
(1)	(2)	(3)	(4)	(5)	(6)
A273	5419.83	5024	3.16	−.83	.07
A273	5421.82	4706	2.01	−1.62	−.02
A277	5419.84	4675	2.64	−.11	.09
A277	5421.83	4473	2.26	−.22	.05
B004	5421.80	3760	1.30	.25	
B009	5421.81	5097	2.97	−.15	.43
B028	5421.84	5566	4.40	.03	.13

Notes.
[a] Uncorrected for phase.

(This table is available in its entirety in machine-readable and Virtual Observatory (VO) forms in the online journal. A portion is shown here for guidance regarding its form and content.)

to make it consistent with the Behlen data and all the data was generally used to obtain the best period. The uncertainty was estimated by plotting the phased light curves and determining the change of period that produces an unacceptable phase match between the two data sets. In doing so, an attempt was made to err on the high side. Light curve scatter, changes in the shape of the light curves and small amplitudes account for most of the unusually large uncertainties. The results are listed in Table 5 where Column 1 gives the running numbers of the stars and Columns 2 and 3 the periods and their uncertainty.

When no period uncertainty is listed the available data were insufficient in number or temporal distribution to allow an estimate of the error or the period is poorly defined and the value listed should be regarded as a typical time scale of the variation. When no period is listed, it indicates that a satisfactory period cannot be found. Footnotes explain the situation in individual cases.

Aliases of similar significance are common due to the limited number of data points, light curve scatter, irregularity or non-repetition in some stars, and, of course, the temporal distribution of the sampling. In particular, the NSVS observations were obtained over the course of one year followed by a gap of at least seven years before the Behlen observations. Furthermore, the latter are generally grouped into several observing seasons at yearly intervals. Under these circumstances, aliases cannot be removed reliably and the periods in the table may be in error by more than the quoted uncertainties when the wrong alias was selected. Most of the time these aliases

Table 3
LICK/IDS Indices on the MILES System

Star	Mid Exposure HJD − 2,450,000	CN_1 -	CN_2	Ca4227	G4300	Fe4383	Ca4455	Fe4531	Fe4668
(1)	(2)	(3)	(4)	(5)	(6)	(7)	(8)	(9)	(10)
A273	5419.83	.131	.115	−.002	5.372	2.298	.117	1.851	.479
A273	5421.82	.090	.083	.062	3.876	2.741	.835	1.575	−.121
A277	5419.84	.128	.151	1.561	5.878	5.649	1.633	3.664	5.223
A277	5421.83	.125	.148	1.383	5.935	5.926	2.204	3.630	5.493
B004	5421.80	.079	.149	3.658	5.647	6.620	5.695	5.187	10.241
B009	5421.81	.306	.336	−.718	6.257	2.901	1.705	2.689	4.918
B028	5421.84	−.004	.017	.791	4.414	3.403	1.459	2.909	2.636

Notes. The online version contains an additional 18 columns to accommodate all of the LICK/IDS indices.

(This table is available in its entirety in machine-readable and Virtual Observatory (VO) forms in the online journal. A portion is shown here for guidance regarding its form and content.)

Table 5
Light Curve Parameters from the Behlen Photometry and Atmospheric Parameters from Spectra

No. (1)	Period (2)	σ_P (3)	$\langle V\rangle$ (4)	$\langle V-R\rangle$ (5)	ΔV (6)	σ_V (7)	$n_{\rm obs}$ (8)	$\langle T_{\rm eff}\rangle$ (9)	$\langle \log\ g\rangle$ (10)	[Fe/H] (11)	E_{V-R} (12)	Notes (13)
B001	1.27259	0.00003	12.91	0.39	0.48	0.014	22					a,d,e
B002	60.65	0.10	12.15	1.54	0.11		5					c
B003	75.8	0.2	13.52	1.28	0.44		6					c,f
B004			12.43	0.98	0.45		8		1.30	0.25		c,d
B005	90		12.14	0.93	0.33		22					c,f,i,j

Notes.
[a] Using the period from Column (2), $\langle V\rangle$ and $\langle V-R\rangle$ are the intensity means over the cycle, ΔV is the amplitude of a Fourier fit to the light curve, and σ_V is the rms scatter of the individual points about the Fourier fit.
[b] The variation in the Behlen data was judged to be of marginal significance. $\langle V\rangle$ and $\langle V-R\rangle$ are the arithmetic means of the nightly mean magnitudes and colors, and σ_V is the rms scatter about the mean magnitude. ΔV is not listed.
[c] This star is a likely variable in the Behlen data but no meaningful period could be determined for the Behlen data, the variation was irregular or the phase coverage of the Behlen data was inadequate for a meaningful Fourier fit. $\langle V\rangle$ and $\langle V-R\rangle$ are the arithmetic means of the nightly mean magnitudes and colors, and ΔV is the range of the observed magnitudes. No σ_V is given.
[d] See Table 11 for a note regarding this star.
[e] Based on the light and color curve this star is possibly an eclipsing binary.
[f] Variable amplitude.
[g] Possibly the mean magnitude varies over hundreds of days based on variations within the NSVS data set or between the NSVS and Behlen data sets.
[h] No period or time scale satisfies all of the data. The best value for the Behlen data is tabulated.
[i] The shape of the light curve varies or there is phase jitter present.
[j] No period or time scale fits all of the data but there are too few data from Behlen to determine them. The overall best value is tabulated and was used in the analysis.
[k] No meaningful period or time scale was found for the Behlen photometry. The tabulated value was derived from the NSVS data only.
[l] Not used.
[m] One or a few anomalous points were omitted from the analysis.
[n] The standard error of the zero point of the magnitudes and/or colors for the comparison stars was between 0.015 and 0.050 mag.
[o] The zero point of the magnitudes and/or colors of the comparison stars was uncertain by more than 0.05 mag due to the availability of only a single photometric night for this field, poor agreement between two photometric nights, or unusual scatter in the magnitudes and/or colors. Hence, the values of the magnitudes and colors in Columns 4 and 5 are of questionable reliability.

(This table is available in its entirety in machine-readable and Virtual Observatory (VO) forms in the online journal. A portion is shown here for guidance regarding its form and content.)

are close together so the cited period is adequate for the purpose of characterizing the behavior of the star (but not phasing observations separated significantly in time). Especially problematic cases are explained in footnotes.

Table 6 lists stars for which different, but well-determined, periods were found for the NSVS and the Behlen data. Most are likely to be due to large period changes over the seven or more years between the two data sets.

4.2. Parameters Derived from the NSVS Data

In analyzing the NSVS data, we adopted the periods from Table 5 except for the stars listed in Table 6 where the periods from Column 2 of that table were used. Parameters determined from the NSVS photometry are listed in Table 1 where Column 4 gives the mean magnitude, $\langle m\rangle$, Column 5, the amplitude or range of the variation, Δm, and Column 6, the scatter of the data points, σ_m. Column 7 lists the number of data points from the NSVS database. The method of determining the first three of these depended on (1) whether the NSVS photometry indicated significant variation, (2) whether the pulsation appeared to be well-behaved, and (3) whether the light curve was well sampled over the cycle. The judgment as to whether there was significant variation was based on a visual examination of the light curve taking into account the brightness of the star, the number of light curve points, the distribution of observations over the cycle and whether the presumptive variability was due a minority of deviant points. While obviously subjective, it is based on experience gained by comparing NSVS light curves with the Behlen photometry. However, the judgment for individual stars was made without reference to the Behlen photometry. Thus, it should not introduce bias into the discussion of the long-term pulsational behavior.

Table 6
Stars with Large Period Changes

Star (1)	$P_{\rm NSVS}$ (2)	$P_{\rm Behlen}$ (3)
B014	24.5	1.2437
B071	75.	86.
B084	68.	42.8
B159	87.	51.
B160	43.7	45.4
B213	66	90.
B214	0.143564	0.174976
B218	93.	140.
B229	69.	130.
B230	40.7	37.2
B257	24.7	13.1
B267	16.	14.1
B278	9.412	9.449
H007	71.	64.
H014	34.3	36.0
H016	6.65	3.54
H087	62.5	32.7
H120	1.5323	1.5327
H137	23.0	22.5
H140	5.1765	3.1835
T003	220.	34.55

If the three conditions of the previous paragraph were met (indicated by footnote a in Column 8 of Table 1), $\langle m \rangle$ is the intensity mean magnitude over the cycle. The amplitude, Δm, and the scatter about the mean light curve, σ_m, were obtained from a Fourier series that was fit to the data. In a few cases of a poor fit due to a rapid rise to maximum, the tabulated amplitude was adjusted appropriately and the poorly fit portions of the light curve were excluded from the determination of the scatter. Note that the light-curve scatter, σ_m, includes photometric error as well as scatter introduced by non-repetition of the light curve over multiple cycles.

If the variation was judged to be of marginal significance (footnote b), $\langle m \rangle$ is the arithmetic mean of the nightly mean magnitudes. Nightly means were averaged since most of the program stars vary little in the course of a single night. σ_m is the rms scatter about the mean magnitude and no amplitude is given.

If significant variation is present but no meaningful period could be determined for the NSVS data, the variation was irregular or the phase coverage of the NSVS data was inadequate (footnote c), $\langle m \rangle$ is again the mean of the nightly means but no value is given for σ_m. In this case the amplitude, Δm, is estimated as the difference between the medians of the five faintest and five brightest data points.

4.3. Parameters Derived from the Behlen Photometry

Table 5 lists parameters derived from the Behlen photometry. Columns 4 and 5 give the mean magnitudes and colors, $\langle V \rangle$ and $\langle V-R \rangle$, while the amplitudes, ΔV, and light-curve scatter, σ_V, are given in Columns 6 and 7. $\langle V \rangle$ and $\langle V-R \rangle$ were determined in the same ways as described for $\langle m \rangle$ in Section 4.2 (as indicated by footnotes a, b, and c in Column 13 of Table 5). Similarly, the calculation of σ_V followed the same procedures used for σ_m. In the case of the amplitude, ΔV, the procedures from Section 4.2 were followed for stars with well behaved variation or no significant variation (indicated by footnotes a or b). When the variations were not well behaved (footnote c) the tabulated ΔV is the full range of the observed values.

There are a few stars that were not found to vary in either the NSVS or the Behlen photometry (footnote b in both Tables 1 and 5). They have been retained here because some are long term variables while those that are actually constant are useful in the comparison of the NSVS photometry to the Behlen observations below.

The photometric errors are dominated by the calibration of the comparison stars. In most cases, it was possible to determine these uncertainties using the scatter among measurements from all of the photometric nights. Generally, these errors are less than 0.015 mag in both $\langle V \rangle$ and $\langle V-R \rangle$. When the larger of the two errors was between 0.015 and 0.050 mag this is indicated by footnote n. If either error was greater than 0.050 mag or could not be calculated because there were only one or two measurements under photometric conditions, the zero points will be uncertain by an unknown amount. These are indicated with footnote o.

In Column 8 we list the number of Behlen observations for each star. When a star turned out to be redder than $\langle V-R \rangle = 1.1$ or when it appeared to be constant, it was dropped from the observing program. This usually became apparent after a few observations and such cases account for most of the stars with fewer than half a dozen observations.

With the large and inhomogeneous sample of stars presented here a variety of issues arise that cannot be captured in the tabulated parameters. Those particular to individual stars are indicated by footnote d and a corresponding note in Table 11 in the Appendix. The light curves of pulsating stars are sometimes similar in appearance to those of eclipsing binaries. In such cases, the color curve is often helpful for distinguishing between them (see Schmidt 1991, Section 4, for example). When an examination of the light and color curves indicated the likelihood of eclipses, the star is flagged with footnote e. Issues related to the long term stability of the pulsation are flagged with footnotes f through k, while shortcomings of the data are indicated by footnotes j through o.

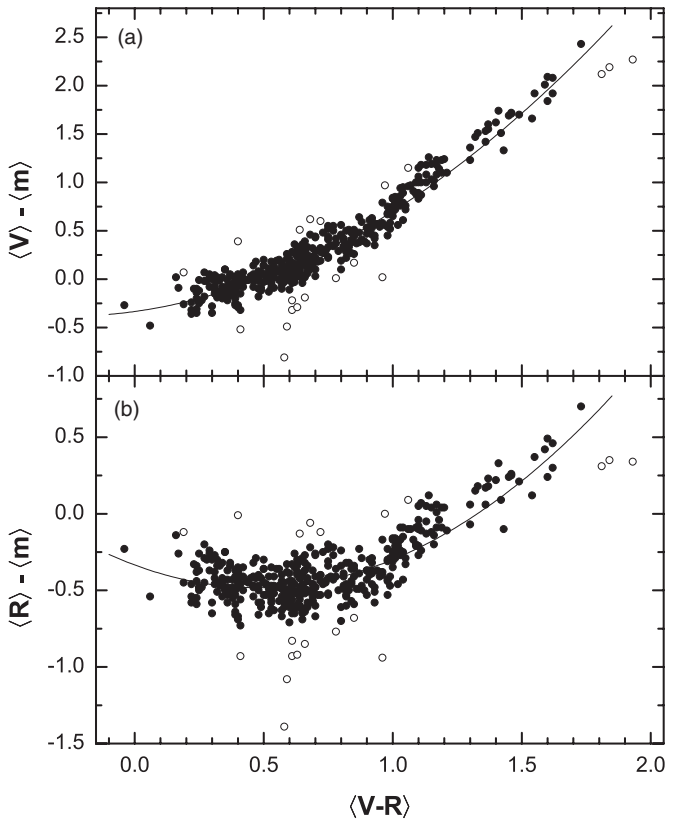

Figure 1. Differences between the Behlen and NSVS magnitudes plotted against the $\langle V-R \rangle$ color. Solid circles represent stars with no evidence for long term variability while open circles depict stars that appear to vary over hundreds of days (identified by footnote g in Table 5). The fitted relations are plotted as solid curves.

4.4. Comparison of the NSVS and Behlen Photometric Systems

While the Behlen photometry employed standard V and R filters and was reduced to the standard VR system as defined by the Landolt (2009) standards, the NSVS photometry was unfiltered. The resulting band pass extends from about 450 to 1000 nm with an effective wavelength similar to the R band (Wozniak et al. 2004).

In Figure 1 we have plotted magnitude differences $\langle V \rangle - \langle m \rangle$ and $\langle R \rangle - \langle m \rangle$ against $\langle V-R \rangle$. As expected, the color effects are considerably smaller in R than in V. The obvious non-linearities reflect the very wide band of the NSVS photometry.

When these plots were originally made, a significant number of outliers appeared above the bulk of the points. In each such case, the field was examined on the finding charts and on images from the STScI Digital Sky Survey.[4] When a second star of significant brightness was found within about

[4] Available at http://stdatu.stsci.edu/dss/.

45″ (the approximate limit for deblending stars in the NSVS, Wozniak et al. (2004)) of the program star it is possible that m is contaminated and the apparent variations spurious. If the Behlen photometry failed to demonstrate significant variation, we concluded that the star is probably constant and it is not listed in Tables 1 and 5. If the Behlen observations showed variability, the star was retained. Such stars are flagged with footnote h in Table 1 but are not plotted in Figure 1. In making this subjective judgment, we tried to err toward marking marginal cases as possibly contaminated.

We fitted the following second order polynomials to the points in Figure 1:

$$\langle V\rangle - \langle m\rangle = -0.334 + 0.374\langle V-R\rangle + 0.661\langle V-R\rangle^2 \quad (3)$$

and

$$\langle R\rangle - \langle m\rangle = -0.334 - 0.626\langle V-R\rangle + 0.661\langle V-R\rangle^2. \quad (4)$$

The standard deviation around both these relationships is 0.15 mag.

We chose to regard stars that scattered from the fitted relation by more than two standard deviations, 0.30 mag, as possibly having changed in mean brightness between the NSVS and the Behlen photometry. Such objects are represented by open symbols in Figure 1 and are flagged with footnote g in Table 5. The circumstances for individual stars are described in notes in Table 11.

Besides long term variations, the combination of the NSVS and the Behlen photometry revealed a variety of other behaviors that were not obvious in the individual data sets. Footnotes to Table 5 indicate their presence.

4.5. Mean Spectroscopic Parameters

The method described in Paper III was used to correct the individual effective temperatures from Table 4 to the cycle means. This method employs the estimated color at the time of the spectrum, $(V-R)_\phi$, and the mean color, $\langle V-R\rangle$. The same values of $(V-R)_\phi$ that were used for calculating the color excesses in Section 3.2 were used here. The means of all the corrected temperatures for each star are listed in Column 9 of Table 5 and constitute our best estimate of the equilibrium temperature, $\langle T_{\rm eff}\rangle$. The estimated uncertainties in $(V-R)_\phi$ were propagated into the temperature correction. If the effect on the overall mean exceeded 75 K no value is listed. Additionally, $\langle T_{\rm eff}\rangle$ was omitted for a few stars due to excessive scatter among the corrected temperatures or lack of a reliable value for $(V-R)_\phi$.

We have no way to correct the gravity for phase and the metallicity and color excess are independent of phase. Thus, simple means of the values from Table 4 are listed in Columns 10, 11, and 12 of Table 5.

5. NEW TYPE II CEPHEIDS

The original motivation for this project was the discovery of new type II Cepheids. Accordingly, we will now discuss the identification of these stars from the complete sample presented in this series of papers. Recalling again that the area of the sky surveyed was restricted so as to exclude classical Cepheids, this discussion only concerns type II Cepheids.

Many other interesting objects have been found and these will be discussed in future papers.

5.1. Stars with Spectra

5.1.1. The Identification of Cepheids

In Paper III, Figure 5(b), we presented a pseudo HR diagram using spectroscopic values of $\langle T_{\rm eff}\rangle$ and $\langle \log\ g\rangle$. In that diagram the stars clearly separated into two regions with a gap between. The adopted dividing line slopped upward to the right from ($T_{\rm eff}\sim 6200$ K, $\log\ g\sim 4.5$) to ($T_{\rm eff}\sim 4550$ K, $\log\ g\sim 0.25$). With a single exception, previously known Cepheids (both type I and type II) fell within the hotter region. We interpreted this to be the Cepheid instability strip. Stars in the cooler region were much more numerous indicating that our photometrically selected sample of Cepheid candidates was heavily contaminated by cooler variables. We also distinguished two groups in the cool region according to gravity but the separation was not as clear and that distinction is of no significance here. Following Paper III, we will refer to stars in the Cepheid region as Cepheid strip stars, and cooler, lower gravity stars as cool sequence stars. Cool stars with higher gravities will be referred to as main sequence stars.

We have located each of the present program stars for which we have at least one spectrum in the pseudo HR diagram and identified those that fall within the Cepheid strip region. For most of the stars, $\langle T_{\rm eff}\rangle$ and $\langle \log\ g\rangle$ from Table 5 were used.

As described in Section 4.5 above, $\langle T_{\rm eff}\rangle$ could not be determined reliably for some stars. Nonetheless, it is still possible to use the temperatures from Table 4 to demonstrate that some are within the Cepheid strip. B036 is too irregular to obtain an estimate of $(V-R)_\phi$ at the time of our only spectrum. However, using the bluest color the star attains will provide a lower limit on the corrected temperature. Since that value still places B036 within the Cepheid strip, it will be considered a Cepheid. The estimated errors in the mean temperatures of B053, B151, B244, B267, and H093, are too large for inclusion in Table 5. However, they are not large enough to move the stars out of the Cepheid strip; accordingly, these stars are also considered Cepheids.

We have listed 30 stars which fall in the Cepheid strip region, including those from Paper III, in Section A of Table 7. These are the most certain type II Cepheids from among our program stars. For each star an approximate period is listed as well as the morphological type of its light curve. The latter is discussed below. The remaining stars were in the cool sequence (defined in Paper III, 283 stars) or the main sequence (53 stars) regions of the pseudo HR diagram.

5.1.2. The Properties of the Spectroscopically Identified Cepheids

Figure 2 compares the distributions of the periods, amplitudes and metallicities of these stars (the upper panels) with stars that were considered to be type II Cepheids by Harris (1985) based on their distances from the Galactic Plane (the lower panels). The periods and amplitudes for panels (b) and (d) were derived from the photometry of Schmidt & Seth (1996) and Schmidt et al. (2004, 2005a, 2005b) except for V833 Oph; unpublished Behlen Observatory photometry was used for that star. Panel (f) is the distribution for the type II Cepheids for which Harris (1981) gave metallicities.

Although the distributions of periods (panels (a) and (b)) may look different to the eye, a Kolmogorov–Smirnov (K-S) test shows that the probability that they were drawn from the same sample is 30%; there is no statistically significant difference between them that would call our identification of type II Cepheids into question.

Table 7
New Type II Cepheids

Star	Period	LC	Star	Period	LC	Star	Period	LC
A. Stars classified on the basis of the spectrum								
A134	1.11	O	H093[a]	1.12	D	A194	1.14	S
A054	1.15	D	A048	1.15	O	A169	1.22	D
R203	1.27	D	A140	1.29	S	A144	1.32	D
B151	1.41	D	A229	1.45	S	A162	1.61	S
A044	1.65	S	A269	1.71	D	B053	2.11	D
A152	2.74	S	A025	2.84	S	R027	2.93	S
H135	3.93	S	A009	4.08	S	A256	4.15	D
A076	4.23	D	A228	8.60	S	A260	10.87	A
A279	11.17	O	B175	12.10	A	B267	14.10	S
B036[b]	30.	D	R125[c]	52.20	S	B244[d]	70.36	A
B. Stars classified on the basis of light curve morphology								
B080[e]	1.15	D	H080[e]	1.35	D	H042[e]	1.67	D
H105[e]	1.89	D	B162[e f]	2.07	D	B243	2.17	D
H106[e]	2.84	D	B123	3.06	D	B070[e]	3.23	D
A240	4.24	D	H012	5.10	D	H148	5.56	D
H072	5.66	D	H098[e g]	15.19	A			
C. Stars classified on the basis of color and/or amplitude								
B138	0.83	D	H091	0.93	O	B008	1.18	B
B105	1.67	O	B114	2.24	S	B109	2.29	S
B142	2.55	S	B050	4.17	O	H076	14.47	A
H050	17.38	O	B170	20.6	S	B067[f]	25.4	S
A071	26.9	S	B111[f]	31.1	O	B155[f]	36.	D
B021[f]	96.	D						

Notes.
[a] This star is V716 Oph, classed as CWB in the GCVS.
[b] This star is LX And, classed as RVB in the GCVS. Due to irregular behavior no period is given in Table 5. A typical time scale is used here.
[c] This star is V480 Lyr, classed as EB: in the GCVS.
[d] This star is V360 Cyg, classed as RVA in the GCVS.
[e] This star also qualified as a Cepheid on the basis of its color and/or amplitude.
[f] This star was considered a non-variable in the Behlen photometry, indicating a large decline in amplitude since the NSVS photometry. It is included here on the basis of its color.
[g] Due to small gaps in the phase coverage for this star, the duration of maximum is uncertain and could exceed 0.3. However, it is included here since the amplitude indicates a Cepheid.

On the other hand, the apparent differences between the amplitude distributions, panels (c) and (d), are supported by the K-S test; the probability that the two were drawn from the same population is a small fraction of a percent. The lack of low amplitude variables in panel (d) likely reflects a bias against their discovery. Since many of the GCVS stars were discovered photographically, this is not surprising. With a larger sample of stars, the conclusion of Paper III that there are a significant number of small amplitude type II Cepheids is strengthened.

A comparison of the metallicities of the present sample with the Harris sample is not straightforward. The distribution of the Harris sample extends to both higher and lower metallicities than that of the present sample. Given the number of stars, the differences at low metallicity are not significant. However, the distributions above about [Fe/H] ~ -1.0 clearly differ. It is likely that this represents a systematic difference in the metallicity scales as a function of metallicity. With this in mind, we note that both data sets indicate that high metallicity type II Cepheids are more common than low metallicity. The medians of both distributions are at the relatively high metallicity of [Fe/H] ~ -0.4.

In Figures 2(e) and (f), the portion of each histogram associated with short-period stars ($P < 8$ days) is hatched. In the lower panel there is an obvious gap in the distribution for short-period stars that is absent in the upper distribution. Some of this may relate to the scale differences alluded to in the previous paragraph but the number of short-period stars in panel (f) is too small to draw a significant conclusion. In any event, our metallicities fail to show any sign of a gap for the short-period stars so we conclude that it is not likely to be a significant feature of these stars.

There are 17 stars with spectra in our program that are included in the GCVS. Four of them, B036 = LX And, B247 = V360 Cyg, H093 = V716 Oph, and R125 = V480 Lyr are in the Cepheid strip region. Their GCVS classifications are CWB, RVA, RVB, and EB:, respectively. Only the uncertain classification for R125 is at odds with their being among the Cepheid strip stars. The other 13 stars are all in the cool sequence according to our spectral classification. One, H126 = V590 Aql, has a GCVS class of RVA which should place it in the Cepheid strip. The other 12 are classed as semi-regular, regular, eruptive, or eclipsing variables; they should not be in the Cepheid strip. We conclude that with only a couple dubious cases out of 17, our spectra have reliably discriminated Cepheids from other stars.

5.2. Stars without Spectra

Since we were unable to obtain spectra for a significant number of our program stars, we examined their photometric properties to identify as many additional type II Cepheids as possible.

5.2.1. Light Curve Morphology

Payne-Gaposchkin (1956) and Kwee (1967) noted that long-period type II Cepheids frequently exhibit flat maxima (called "flat topped" by Kwee) or a significant bump after maximum (Kwee's "crested" light curves). Following from this Schmidt et al. (2004) denoted light curves with flat maxima and rather narrow, symmetric minima as type A while the crested light curves were referred to as type B. An additional group with a bump prior to maximum was designated as type C. The light curves of both type I and type II Cepheids commonly exhibit a rapid rise and slow decline (Schmidt et al. 2005a). These were designated type D light curves by Schmidt et al. (2004) and resemble those of the type ab RR Lyrae stars. These four types are illustrated by examples from the present sample in Figure 3 as well as by examples from Schmidt et al. (2004) and from Paper III.

The light curves of many stars in our sample do not differ at a statistically significant level from sinusoids. We have denoted such light curves as type S. Light curves that could not be placed in any of these categories are referred to here as type O.

We examined the Behlen light curve of each star for which we have a spectrum and assigned a light curve type to it. In a few ambiguous cases, the NSVS and ASAS photometry was also consulted.

It is well known that light curve morphology differs between short- and long-period type II Cepheids. Accordingly, we will discuss the light curve morphology of stars with periods shorter than 8 days separately from those with longer periods. Table 8 lists the number of stars for each light curve type and each region of the $T_{\rm eff}$–log g diagram for the short- and long-period stars.

Short-period Stars. We have spectra for a total of 137 program stars with periods less than 8 days and reasonably regular pulsation. The spectra place 22, 84, and 31 of them, respectively,

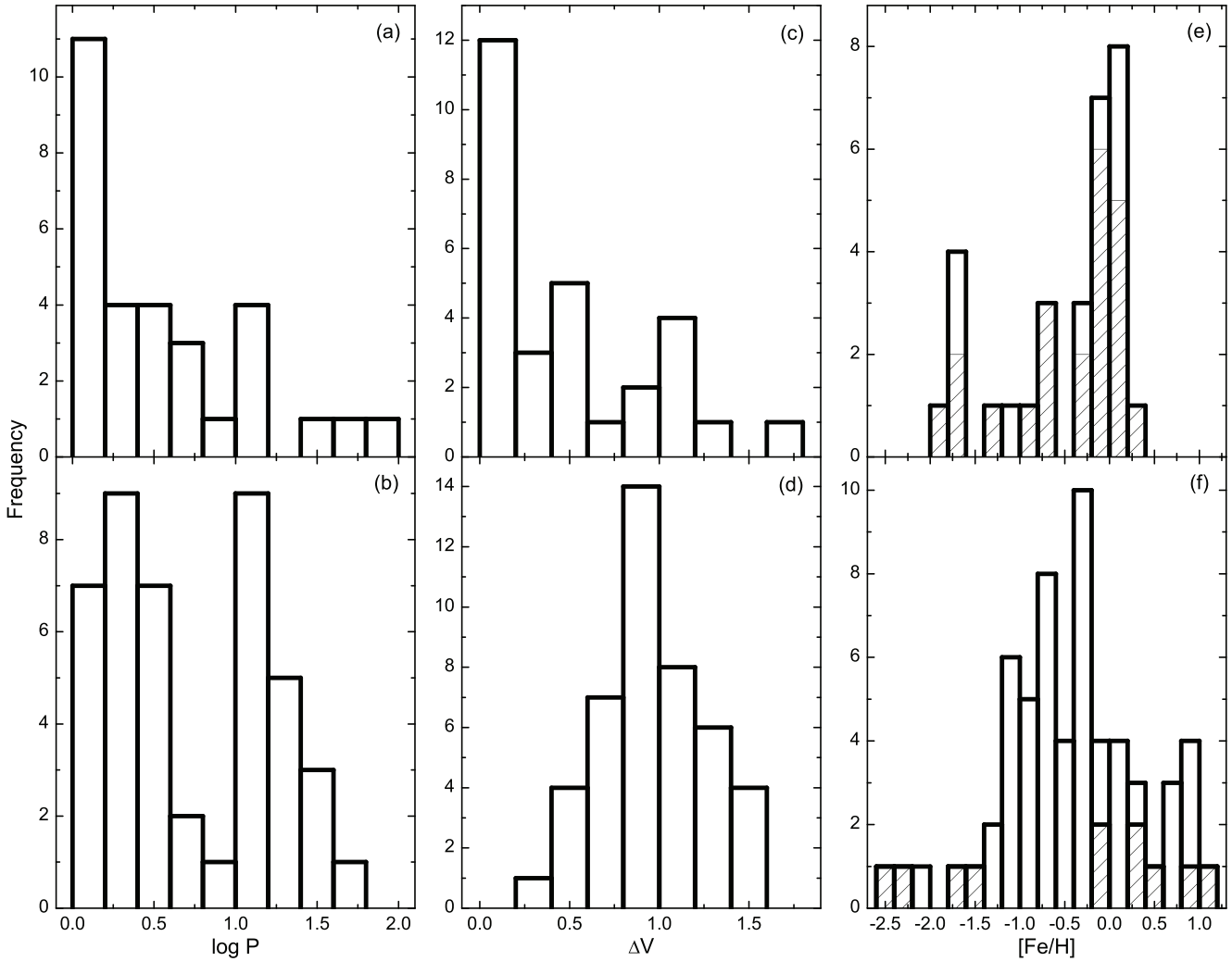

Figure 2. Frequency distributions of the periods, amplitudes and metallicities of type II Cepheids. Panels (a), (c), and (e) represent the present spectroscopically selected sample (listed in Section A of Table 7). Panels (b), (d), and (f) represent known type II Cepheids. In panels (e) and (f) the portion of the histograms representing short-period Cepheids is hatched.

in the Cepheid strip, the cool sequence and the main sequence regions of the pseudo HR diagram. It can be seen in Table 8 that nearly half of the Cepheid strip stars have type D light curves. On the other hand, the only two non-Cepheid strip stars, R047 ($P = 6.36$ days) and R056 ($P = 7.87$ days), both in the cool sequence, exhibit type D light curves.

Additionally, we obtained spectra of 34 known Cepheids in the same period range, all of which fall in the Cepheid strip. They are listed in Sections A and B of Table 9. Most of these stars have type D light curves. We have included type I Cepheids in this list for completeness but none of our conclusions would be altered by omitting them.

The period range of the short-period type II Cepheids in Tables 7A and 9A and the fact that the only two non-Cepheids with type D light curves have periods greater than 6.36 days lead us to we conclude that our Cepheid candidates with periods between 1.11 and 6.17 days and type D light curves can be considered highly likely type II Cepheids.

We examined the light curves of all the short-period stars in our program that lacked spectra. Those with unambiguous D-type light curves, and 1.11 days $\leqslant P \leqslant$ 6.17 days are listed in Section B of Table 7 as short-period Cepheids.

Stars with type S light curves are prevalent in all three regions of the pseudo HR diagram; we will not be able to distinguish Cepheids with sinusoidal light curves photometrically. The resulting incompleteness affects the small amplitude stars disproportionately. Finding the remaining Cepheids must await the availability of suitable spectra.

Long-period Cepheids. We have spectra for 229 program stars with periods longer than eight days. The spectra place 8, 199 and 22 of them in the Cepheid strip, the cool sequence and the main sequence, respectively. There are also 11 known type I and 8 known type II Cepheids in this period range for which we have spectra (listed in Sections A and B of Table 9). All fall in the Cepheid strip.

In the lower section of Table 8 it can be seen that the light curve types found among the Cepheid strip stars are also common among the cool sequence stars. While a closer examination of the type D light curves revealed no obvious way to distinguish the Cepheid strip stars, the A, B, and C stars were more promising.

An examination of Figure 3 suggests that types B and C light curves often represent variations of type A in which the region around maximum is sloped but relatively linear. This is particularly evident when the minimum is symmetric and clearly delimited by inflections. Thus, we will treat the three types together.

Since the Cepheids generally had shorter linear segments around maximum light than the cool sequence stars, we

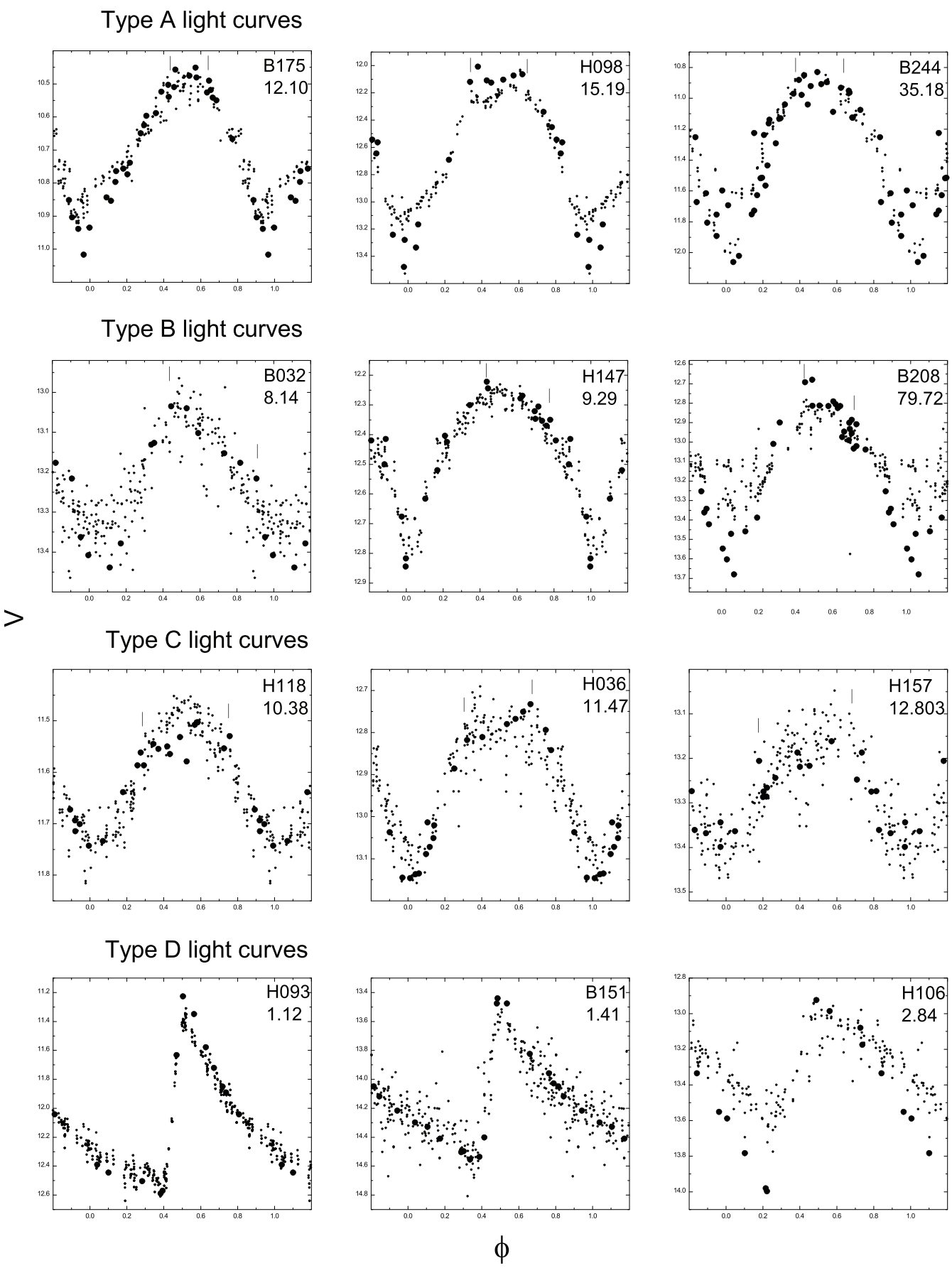

Figure 3. Examples of light curves from the present sample that illustrate the four types of light curves. Large and small symbols represent the Behlen and NSVS photometry, respectively. The phases have been arbitrarily shifted to show the shape of the maximum. The vertical dashes above each light curve in the upper three rows show the region measured to determine $W_{\rm mx}$.

Table 8
Distribution of Program Star Light Curve Types among Regions of the HR Diagram

Light Curve Type	Cepheid Strip	Cool Sequence	Main Sequence
Short-period Stars			
A	...	5	6
B	...	5	1
C	...	2	...
D	10	2	...
S	11	49	24
O	2	20	...
Long-period Stars			
A	3	28	1
B	...	6	...
C	...	3	...
D	1	31	2
S	3	93	15
O	1	38	4

Table 9
Known Cepheids

Star	Period	LC	Star	Period	LC	Star	Period	LC
A. Known type II Cepheids with Spectra								
SW Tau	1.58	D	V971 Aql	1.62	D	UY Eri	2.21	D
V484 Mon	3.14	D	DQ And	3.20	D	BD Cas	3.65	S
V572 Aql	3.77	S	AM Cam	4.00	D	TX Del	6.17	D
IX Cas	9.15	S	AL Vir	10.31	D	QQ Per	11.19	D
V2338 Oph	13.66	C	CS Cas	14.73	B	SZ Mon	16.33	A
TW Cap	28.56	B						
B. Known type I Cepheids with Spectra								
FF Aur	2.12	D	BB Gem	2.31	D	EW Aur	2.66	D
NY Cas	2.82	S	FT Mon	3.42	D	EF Tau	3.45	D
BF Cas	3.63	D	CZ Cas	5.66	D	AP Cas	6.85	D
BB Her	7.51	D	CD Cas	7.80	D	CN Cep	9.50	A
AN Aur	10.29	C	AD Cam	11.26	D	V916 Aql	13.44	D
CH Cas	15.09	D	OT Per	26.09	D	V609 Cyg	31.09	D
C. Known type II Cepheids without Spectra								
V775 Oph	12.18	A	AL Lyr	12.98	A	V801 Aql	14.16	A
V845 Her	15.50	A	V478 Oph	16.35	A	MZ Cyg	21.41	A
PP Aql	24.05	A	CC Lyr	24.23	D	NN Vul	30.82	D
IU Cyg	31.35	B	ET Vul	53.49	A			

measured the phase interval between the inflection points that define them, denoted to by $W_{\rm mx}$. This is illustrated in Figure 3 where the intervals corresponding to the maximum region are indicated by vertical lines. To supplement the small number of Cepheids in the present sample, we also determined $W_{\rm mx}$ for long-period Cepheids from Schmidt et al. (2004) for which we have no spectra (listed in Section C of Table 9). Since these stars are all well known Cepheids, we will assume they are bona fide members of the class.

In Figure 4, $W_{\rm mx}$ is plotted against the period for all these stars. A clear separation is evident between the Cepheids and the other stars; regarding stars with $W_{\rm mx} \leqslant 0.3$ as Cepheids will result in few false positives and will exclude few Cepheids. The variables in Figure 4 have periods between 9.5 and 70.4 days so this criterion should only be applied in that range.

We examined the light curves of all the long-period stars that lacked spectra and determined $W_{\rm mx}$ for those with type A, B or C

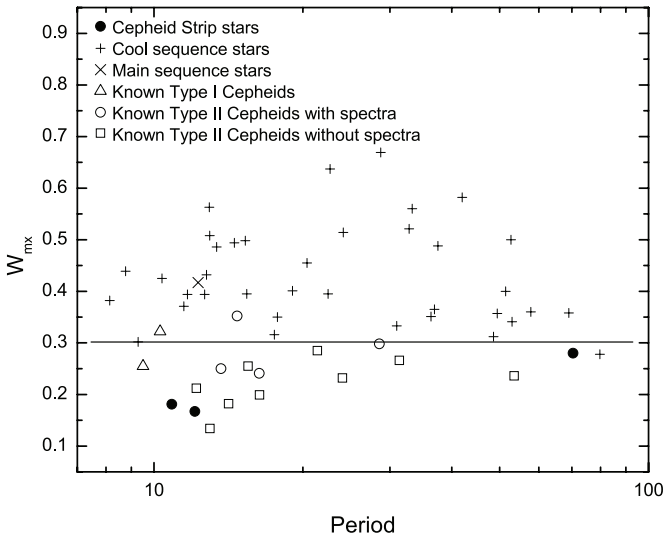

Figure 4. Width of the light curve maximum, $W_{\rm mx}$, plotted against period for stars with A, B, or C light curves. Filled circles represent program stars in the Cepheid strip, plus signs represent stars in the cool sequence, Xs denote main sequence stars, open circles represent known type II Cepheids with spectra, open triangles represent known type I Cepheids with spectra, and open squares represent type II Cepheids from Schmidt et al. (2004) for which we lack spectra. As discussed in the text, the horizontal line represents the adopted division between Cepheids and non-Cepheids.

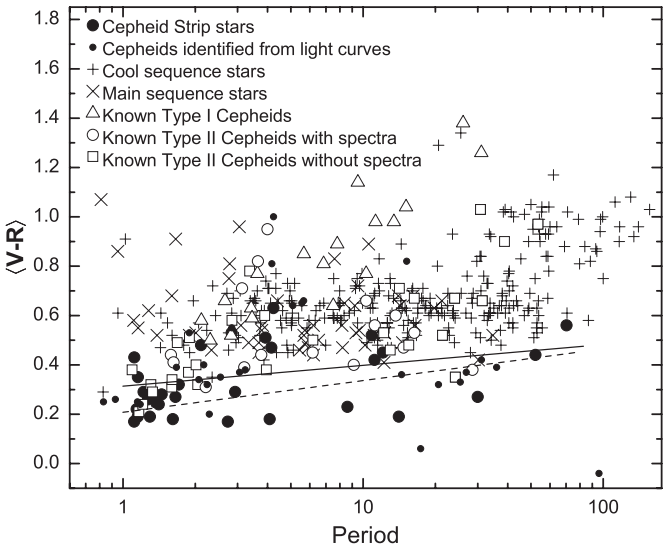

Figure 5. Mean color, $\langle V-R \rangle$, plotted against the period. The symbols have the same meaning as in Figure 4 with the addition of small filled circles to represent stars listed in parts B and C of Table 7. The solid line separates the upper region containing Cepheid strip, cool sequence, and main sequence stars from the lower region containing only Cepheids as discussed in the text. The dashed line is the lower boundary of the Cepheid region originally identified in Figure 2 of Paper I.

light curves. Only one star, H098, met the criteria in the previous paragraph and it is listed in Section B of Table 7. Although the light curves of long-period stars produced only one additional Cepheid, this criterion will be useful in future studies of these stars. Again some Cepheids have certainly been missed. Spectra are needed to rectify this.

5.2.2. Colors and Amplitudes

In Figure 5, the mean color, $\langle V-R \rangle$, is plotted against the period for all of the stars with spectra and known type II Cepheids

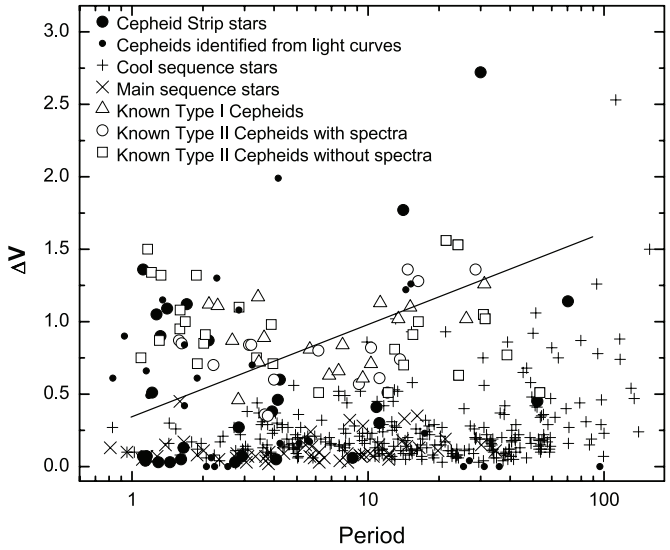

Figure 6. Amplitudes, ΔV, plotted against the period. The symbols have the same meaning as in Figure 5. The solid line separates the lower region where Cepheids, cool sequence stars and main sequence stars are found from the upper region with only Cepheids as discussed in the text.

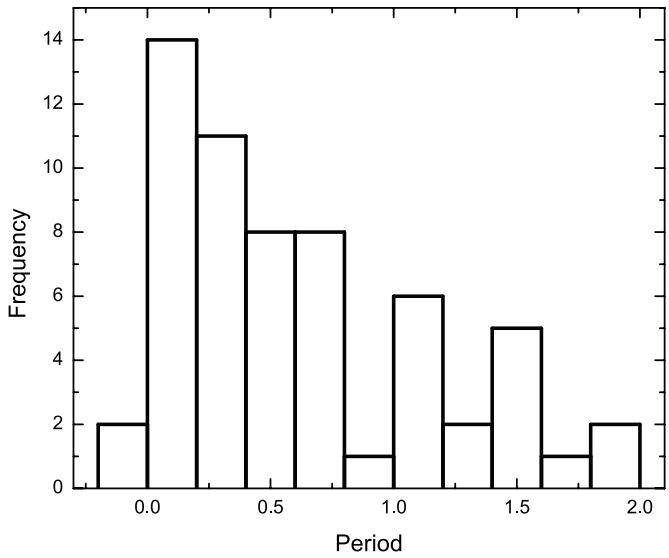

Figure 7. Frequency distribution of the periods of all the stars in Table 7.

from Schmidt et al. (2004, 2005a, 2005b). For $\langle V-R\rangle \gtrsim 0.4$ the Cepheids are mixed with the cool sequence and main sequence stars while at bluer colors the latter are largely absent. We have drawn a line separating the two regions defined by

$$\langle V-R\rangle = 0.32 + 0.08\ \log P \tag{5}$$

and will consider stars below it to be Cepheids.

In Figure 6, the amplitude, ΔV, is plotted against period for the same stars. In this case, the various types of stars are mixed at lower amplitudes but only Cepheids are found above the solid line defined by

$$\Delta V = 0.35 + 0.64\ \log P. \tag{6}$$

Stars above this line will be considered Cepheids.

A number of the Cepheids identified by light curve morphology are also Cepheids based on one or both of these criteria. These stars are identified by footnote e in Table 7. Other stars that meet one or both of these criteria are listed in part C of Table 7. In Figures 5 and 6 the stars from parts B and C of Table 7 are shown by small symbols for reference. Both of these criteria are valid in the range from about 0.8 to 100 days. Again, we emphasize that this selection is incomplete since many Cepheids fall among the other stars in Figures 5 and 6.

5.3. Properties of the Sample

Although the list of Cepheids in Table 7 is far from complete and some are uncertain members of the class, a few comments about them are in order.

Figure 7 shows the period distribution for all of stars listed in Table 7. Even though the number of stars has doubled from those plotted in Figure 2(a), the distribution has not changed within the statistical uncertainties; the K-S test is still inconclusive regarding the similarity to Figure 2(b). Again, the period distribution does not call into question the identification of the Cepheids in Sections B and C of Table 7.

There are five stars for which the amplitudes diminished between the NSVS and the Behlen observations to the point where they were no longer considered variable; they are flagged with footnote e in Table 7.[5] With a single exception, B162, all have periods in excess of 25 days. This suggests that intermittent pulsation may be common among the longer period, more luminous type II Cepheids or RV Tau stars. However, further investigation, particularly spectra, are needed to firmly establish the nature of these objects.

There is an apparent sequence of stars in Figure 5 from roughly ($P = 2.7$ days, $\langle V-R\rangle = 0.17$) to ($P = 30$ days, $\langle V-R\rangle = 0.27$). The bluest stars with periods between one and two days lie on an extension of this sequence and probably should be considered part of it as well. Two other stars, H050 at ($P = 17.38$ days, $\langle V-R\rangle = 0.06$) and B021 at ($P = 96$ days, $\langle V-R\rangle = -0.04$), lie well below the sequence. All of these objects are bluer than the dashed line that was used in Paper I as a preliminary blue limit for type II Cepheids. Most have spectra that yielded temperatures hotter than 7000 K and gravities around $\log g = 4$. This places them hotward and below of most of the program stars in the HR diagram (see Figure 5(b) of Paper III). It is unclear whether they constitute a separate group of stars and, thus, another type of object, or are simply the hottest of the type II Cepheids. They clearly deserve further study and future paper is planned that will explore their nature.

5.4. Comparison with MACC Classifications

The Machine-learned ASAS Classification Catalog (MACC; Richards et al. 2012) presented physical classifications for about 50,000 variables. The training set for the machine learning procedure was composed of a large number of stars with established membership in 28 different variable star classes.

We have spectra for 174 stars from the MACC. In Table 10 we list the numbers of these stars in each MACC class. The second through the fourth columns give the numbers for our three regions of the HR diagram while the fifth through the tenth columns break them out according to our light curve types.

Looking first at the left-hand portion of the table, we note that the 20 ASAS stars that were placed in the Cepheid strip by our spectra are scattered among nine MACC classes.

[5] Stars were selected for spectra on the basis of the existing Behlen photometry. Stars with no apparent variation were given low priority so there is no significance to the fact that this group includes only stars without spectra.

Table 10
Comparison of Present Classifications with MACC[a]

MACC Class	Cepheid Strip	Cool Sequence	Main Sequence	A	B	C	D	S	O	Phot. Class
Mira	...	...	...	...	...	...	...	...	...	...
Semireg PV	...	2(1)	...	...	...	...	1(0)	...	1(1)	...
SARG A	...	2(0)	2(1)	1(0)	...	...	...	3(1)	...	...
SARG B	...	11(2)	...	2(0)	...	...	1(1)	6(1)	2(0)	...
LSP	...	2(0)	...	...	...	...	...	2(0)	...	...
RV Tauri	...	5(1)	...	1	...	...	...	2(0)	2(0)	...
Classical Cepheid	2(1)	3(0)	...	...	...	...	2(1)	1(0)	2(0)	2
PopII Cepheid	...	1(0)	...	...	...	...	...	...	1(0)	2
Multi-Mode Cepheid	1(0)	8(1)	...	...	1(1)	...	2(0)	5(0)	1(0)	1
RR Lyrae FM	3(2)	...	...	...	...	...	3(2)	...	...	2
RR Lyrae FO	...	...	...	...	...	...	...	...	...	...
RR Lyrae DM	...	...	...	...	...	...	...	...	...	...
Delta Scuti	1(0)	...	...	...	...	...	...	1(0)	...	...
SX Phe	...	...	...	...	...	...	...	...	...	...
Beta Cephei	...	...	...	...	...	...	...	...	...	...
Pulsating Be	1(0)	...	...	...	...	...	...	...	1(0)	...
RSG	...	...	...	...	...	...	...	...	...	...
Chem Peculiar	4(0)	1(1)	...	...	...	...	1(1)	3(0)	1(0)	...
RCB	...	...	...	...	...	...	...	...	...	...
Class T Tau	...	...	...	...	...	...	...	...	...	...
Weak-line T Tau	4(2)	74(45)	25(16)	13(6)	5(3)	2(2)	8(4)	62(39)	13(9)	4
RS CVn	...	6(0)	1(0)	...	...	...	1(0)	5(0)	1(0)	...
Herbig AEBE	...	1(0)	...	...	...	...	...	1(0)	...	...
S Doradus	...	...	...	...	...	...	...	...	...	...
Ellipsoidal	...	...	...	...	...	...	...	...	...	...
Beta Persei	2(0)	2(1)	...	...	...	...	...	2(0)	2(1)	...
Beta Lyrae	...	3(0)	...	...	...	...	...	3(0)	...	...
W Ursae Maj	2(0)	5(1)	...	2(0)	1(0)	...	...	2(0)	2(1)	...
Total	20(5)	126(53)	28(17)	19(7)	7(4)	2(2)	19(9)	98(41)	29(12)	11

Note. [a] The numbers in parentheses refer to stars with classification probabilities greater than 0.50.

Conversely, there are 17 stars in our cool sequence with MACC classifications that should place them in the Cepheid strip (Classical Cepheid, Pop II Cepheid and Multi-Mode Cepheid and RV Tauri). This reflects the difficulties we encountered using light curves to separate the Cepheids from the cooler stars and supports our conclusion that light curves are often insufficient for determining the physical nature of stars in the Cepheid period range. On the other hand, the situation appears to be more favorable for the cooler stars. Most stars classed as Semireg PV, SARG A, SARG B, LSP, and Weak-line T Tau fall in the cool sequence or main sequence as they should.

The correspondence between our light curve types and the MACC classifications is surprisingly poor. The Weak-line T Tau stars are distributed among all of our light curve types while we have no stars in the Class T Tau class. Our type S light curves are spread across a dozen MACC classes. This is perplexing since both classifications are based on light curves.

The MACC classifications are accompanied by an estimate of the probability that an object is a member of the assigned class. For many of our stars the probabilities are relatively low with a median value of 0.42. To determine whether low probability classifications influence the distribution of stars in Table 10, we list the numbers for stars with probabilities exceeding 0.5 in parentheses. While there may be some small improvements in the distributions, they are not statistically significant given the smaller number of objects. We conclude that low probability classifications are not the cause of the discrepancies discussed above.

A possible cause of these discrepancies is the inclusion of faint stars where the ASAS light curves become increasingly scattered. However, the median magnitude of the stars represented in Table 10 is relatively bright at $V = 11.4$ and there are only four stars fainter than $V = 13$. Furthermore, a plot of the classification probability against the magnitude shows no correlation. We conclude that the inclusion of faint stars does not affect this discussion.

An examination of the NSVS, ASAS, and Behlen photometry suggests several factors that may be relevant. (1) Significant intrinsic scatter occurs in some of the light curves, up to $\sigma_V = 0.08$ mag. (2) Many of the stars have small amplitudes with a median of $\Delta V = 0.14$ mag. At small amplitude, light curve features are less easily determined in the presence of scatter and light curves often tend toward sinusoids. (3) The period or light curve shape changes over time in some stars. These issue clearly merit further investigation but fall outside the scope of this paper.

In the last column of Table 10, we give the distribution of stars identified from the photometry as type II Cepheids (listed in Sections B and C of Table 7) among the MACC classes. The sample is much too small to allow any conclusion to be drawn but the number classed as Weak-line T Tau stars in the MACC is a source of some concern.

The comparison with the MACC confirms the difficulty of using light curves for identifying Cepheid strip stars even when large data sets and sophisticated analysis techniques are used. It appears that the light curves simply lack the needed information.

However, this does not detract from the importance of efforts to classify light curves automatically. These techniques are necessary to characterize the statistical properties of the large samples of variable stars being discovered in surveys and to identify interesting stars for more detailed study. They will only increase in importance as photometric databases grow ever larger.

6. CONCLUSIONS

This is the last paper in this series and the following conclusions pertain to the results from all four of the papers in this series:

1. We identified 934 Cepheid candidates, mostly from the NSVS. New photometric observations are presented for all them and spectral observations for about 40% of them.
2. Thirty new type II Cepheids were identified using spectra. Most of the stars with spectra proved to be cooler stars scattered along the red giant branch (283 stars) and main sequence (53 stars).
3. Among the stars that lack spectra, 14 new type II Cepheids were identified on the basis of their light curves and 16 on the basis of colors and/or amplitudes. In many cases these criteria do not distinguish between Cepheids and cooler variables so we anticipate that other type II Cepheids remain undetected in our sample.
4. Low amplitude type II Cepheids are rather common. Half of our sample with spectra have amplitudes smaller than $\Delta V = 0.4$.
5. There is an apparent sequence of variables blueward of the known type II Cepheids, and two additional stars with Cepheid-like periods but even bluer colors.
6. The number of type II Cepheids is much smaller than our original estimates based on the number of such stars known in globular clusters. Although the detection of Cepheids in our sample is clearly incomplete, this does not account for the small number found.
7. A sizable fraction of type II Cepheids have metallicities near solar with [Fe/H] > -0.4. The distribution is quite different from the globular cluster Cepheids.
8. Based on the last two points, the original assumption that field type II Cepheids are related to similar stars in globular clusters is clearly incorrect. This raises the question of their origin as well as the question of why the halo does not contain a larger number of Cepheids that have escaped from globular clusters.

Some of the observations were taken by student observers Brian Hemen, Shawn Roberts, Danielle Rogalla, Lauren Thacker-Lynn, and Ethan VanWinkle. Their contributions to this project are gratefully acknowledged. Helpful comments by Joseph Richards concerning the MACC classifications are greatly appreciated. This publication makes use of the data from the Northern Sky Variability Survey created jointly by the Los Alamos National Laboratory and University of Michigan. The NSVS was funded by the Department of Energy, the National Aeronautics and Space Administration, and the National Science Foundation. Equipment used in the observations was purchased with funds from NSF grant AST 00-97353. I am grateful to the Department of Physics and Astronomy at the University of Nebraska for continued support for the operation of Behlen Observatory. I wish to thank the staff members of Kitt Peak National Observatory for their very able help in obtaining the spectra used here.

Facility: KPNO:2.1m

APPENDIX

Table 11
Notes on Individual Stars

Number	Note
A272	The photometric parameters for this star were taken from Schmidt et al. (2009).
A277	The photometric parameters for this star were taken from Schmidt et al. (2009).

(This table is available in its entirety in machine-readable and Virtual Observatory (VO) forms in the online journal. A portion is shown here for guidance regarding its form and content.)

REFERENCES

Akerlof, C., Amrose, S., Balsano, R., et al. 2000, AJ, 119, 1901
Ferraz-Mello, S. 1981, AJ, 86, 619
Harris, H. C. 1981, AJ, 86, 719
Harris, H. C. 1985, AJ, 90, 756
Hoffman, D. I., Harrison, T. E., & McNamara, B. J. 2009, AJ, 138, 466
Kwee, K. K. 1967, BAN, 19, 260
Landolt, A. U. 2009, AJ, 137, 4186
Mondal, S., Lin, C. C., Chen, W. P., et al. 2010, AJ, 139, 2026
Payne-Gaposchkin, C. 1956, VA, 2, 1142
Pojmanski, G., Pilecki, B., & Szczygiel, D. 2005, AcA, 55, 275
Richards, J. W., Starr, D. L., Miller, A. A., et al. 2012, ApJS, 203, 32
Schmidt, E. G. 1991, AJ, 102, 1766
Schmidt, E. G., Hemen, B., Rogalla, D., & Thacker-Lynn, L. 2009, AJ, 137, 4598 (Paper II)
Schmidt, E. G., Johnston, D., Langan, S., & Lee, K. M. 2004, AJ, 128, 1748
Schmidt, E. G., Johnston, D., Langan, S., & Lee, K. M. 2005a, AJ, 129, 2007
Schmidt, E. G., Johnston, D., Langan, S., & Lee, K. M. 2005b, AJ, 130, 832
Schmidt, E. G., Langan, S., Rogalla, D., & Thacker-Lynn, L. 2007, AJ, 133, 665 (Paper I)
Schmidt, E. G., Rogalla, D., & Thacker-Lynn, L. 2011, AJ, 141, 53 (Paper III)
Schmidt, E. G., & Seth, A. 1996, AJ, 112, 2769
Skrutskie, M. F., Cutri, R. M., Steining, R., et al. 2006, AJ, 131, 1163
VandenBerg, D. A., & Clem, J. L. 2003, AJ, 126, 778
Wils, P., & Greaves, J. 2004, IBVS, 5512, 1
Wozniak, P. R., Vestrand, W. T., Akerlof, C. W., et al. 2004, AJ, 127, 2436